www.czasopisma.pan.pl PAN POLSKA AKADEMIA NAUK www.journals.pan.pl

Arch. Metall. Mater. **68** (2023), 4, 1429-1438

DOI: https://doi.org/10.24425/amm.2023.146209

S. KAILAINATHAN[1], M. EZHILAN[1], S.V. ALAGARSAMY[2*], C. CHANAKYAN[3]

INVESTIGATIONS ON TRIBOLOGICAL BEHAVIOUR OF TITANIUM DIOXIDE PARTICLES FILLED Al-0.6Fe-0.5Si ALLOY COMPOSITE USING TOPSIS APPROACH

Aluminium metal matrix composites (AMMCs) playing a prominent part in the aerospace and automotive sectors owing to their superior mechanical and tribological properties. Hence, the aim of this work is to investigate the effect of titanium dioxide (10 wt.% TiO_2) particles addition on hardness and tribological behaviour of Al-0.6Fe-0.5Si alloy (AA8011) composite manufactured by stir casting method. The surface morphology of developed composite clearly shows the inclusion of TiO_2 particles evenly distributed within the matrix alloy. Hardness of the composite was measured using Vickers micro hardness tester and the maximum hardness was obtained at 95.6 Hv. A pin-on-disc tribometer was used to carried the wear test under dry sliding conditions. The influence of wear control parameters such as applied load (L), sliding speed (S) and sliding distance (D) were taken as the input parameters and the output responses considered as the specific wear rate (SWR) and co-efficient of friction (COF). The experimental results were analyzed using Technique for Order Preference by Similarity to Ideal Preferred Solution (TOPSIS). Based on the TOPSIS approach, the less SWR and COF achieved at the optimal parametric combination were found to be L = 30 N, S = 1 m/s and D = 2000 m. ANOVA results revealed that applied load (76.01%) has the primary significant factor on SWR and COF, followed by sliding speed (20.71%) and sliding distance (3.12%) respectively. Worn surface morphology was studied using SEM image of confirmation experiment specimen to understand the wear mechanism.

Keywords: Al-Fe-Si alloy; TiO_2; Stir casting; Hardness; Tribological behaviour and TOPSIS

1. Introduction

Aluminium alloys and its matrix composites are focused with superior concern to produce light weight structures and advanced load bearing capacity which is higher strength when compared to the base metals. Generally, the blending of one or more classified materials is conventional to compile the composites with proper reinforcement and parent material [1]. In this composite, reinforcement phase and continuous phases are categorized. Next to classify the other various types like metal matrix composites, ceramic matrix and polymer matrix [2]. Aluminium matrix composites (AMCs) are widely utilized in aerospace, automotive, ship building and aircraft sectors [3]. Particularly, the AMCs have high potential strength, superior mechanical and tribological performances, produce greater stability machineries with combination of low weight and high strength ratio [4]. Similarly, AMCs also achieves the better alternate and greater life in manufacturing of brake drum, cylinder blocks, pistons, brake lining and clutches in automotive sectors. The composed AMCs enhancing the mechanical characterization with prominent ductility due to mechanical deformation are highly influenced [5]. From the last two decades, the firms fully concentrated on the high strength, resist wearing, resisting to corrosion and greater thermal stability materials are employed to generate the machinability parts [6]. Based on above the summarized statements, therefore this research selected AA8011 (Al-0.6Fe-0.5Si) as a base material. Usually, AA8011 possess major constituents of Fe-Si, these intermetallic elements which led to enhance the age hardening attributes. There is a reason for choosing AA8011 is microstructure refinement will be developed homogeneously with the influence of significant mechanical attributes and also the cost is less. Based on the desired applications, the reinforcements were utilized with different choices to base matrix of aluminium [7]. The reinforcement volume fractions and the essential properties of aluminium is a major significant role to fabricate the AMCs with superior mechanical characteristics. It is revealed that the interface bonding between the aluminium matrix and reinforcement is a vital

[1] ROHINI COLLEGE OF ENGINEERING AND TECHNOLOGY, DEPARTMENT OF MECHANICAL ENGINEERING, KANYAKUMARI-629 401, TAMIL NADU, INDIA
[2] MAHATH AMMA INSTITUTE OF ENGINEERING AND TECHNOLOGY, DEPARTMENT OF MECHANICAL ENGINEERING, PUDUKKOTTAI-622 101, TAMIL NADU, INDIA
[3] RVS COLLEGE OF ENGINEERING AND TECHNOLOGY, DEPARTMENT OF MECHANICAL ENGINEERING, COIMBATORE-641 402, TAMIL NADU, INDIA

* Corresponding author: s.alagarsamy88@gmail.com

role. Most of the literatures focused on various reinforcements like SiC, CNTs, B_4C, MoS_2, Al_2O_3, Gr, etc. [8]. From these reinforcements TiO_2 are a better combination to employ with AA8011 and it diminishes the complex layer of surface and greater interfacial bonding is attained. Next the processing method is major key roles to produce the defect free AMCs. Therefore, the stir casting technique is a healthier process to resolving the pitiable wetting along with ceramic and matrix reinforcements when non homogeneous scattering is created. This method is most opt route for fabrication of AMCs due to their simplicity, most economical, flexibility and mass production [9-10]. The combinations of AA8011 and TiO_2 AMCs were not yet discussed more in earlier researches. Alagarsamy et al. [11] studied the properties of AA7075 matrix composites filled with TiO_2 particles fabricated through stir casting route. They observed that the hardness, tensile strength and wear resistance drastically increased with an increase in TiO_2 content up to 10 wt.% after that slightly decreased. Tetsuro et al. [12] fabricated the two metal-core piezoelectric fibers to measure the viscosity and temperature. Those materials are composed with metal matrix composites integrated with oxide metal fiber and metal core fiber. Finally the multifunctional material was successfully fabricated by MMCs. Min et al. [13] synthesized the ADC12 alloy with TiO_2 reinforcement and coated CNTs to produce the AMCs. The TiO_2 improves the wettability of carbon nanotubes to aluminium. The better interfacial bonding was created between the base and reinforcement by the influence of TiO_2. Prabhu et al. [14] fabricates the AMCs with AA6061 and rutile particles having various reinforcement weight fractions. They noticed that, when utilizing the 3 wt.% of reptile particles tensile strength was diminished. Ramkumar et al. [15] investigated the impact of TiO_2 on pure aluminium by accumulative roll bonding technique to improve the homogeneous dispersion and mechanical behaviour. By the increment of TiO_2 reduces the grain sizes to exhibit the tensile and hardness in increasing manner. David et al. [16] synthesized the AMCs between the AA6061, SiC and fly ash particles by stir casting process. Mechanical and microstructure characterization were improved by the fabricated AMCs. The homogeneous dispersion was attained on the AMCs by the SEM analysis. Samuel O. Akinwamide [17] developed SiC incorporated aluminium composites and observed that inclusion of SiC improved the hardness and formation of the oxide layer decreases the WR. Jaswinder et al. [18] fabricated the AMCs by the presence of AA2024, SiC and red mud particles by using stir cast method. The density and porosity was diminished with added of reinforcements on the base alloy with proper setting of casting parameters. Similarly, the strength was accomplished by increasing 34 percentages to the base alloy. Roshan Xavier et al. [19] investigated the mechanical and wear properties of AA7050-TiO_2 composites fabricated via liquid metallurgy route and they reported that the tensile strength, hardness and wear resistance improved up to 5 wt.% TiO_2 addition. Raju et al. [20] fabricated the lithium and silicon nitride content incorporated with Al2024 MMCs and studied the dry sliding behaviours using pin on disc tribometer. They revealed that the WR reduced by increase in load and sliding speed and also reported that wear resistance improved due to formation of MML which is induced by inclusion of hard reinforcement particles. Nenad Miloradovic et al. [21] studied the effect of dry sliding wear control parameters for SiC and Gr particles reinforced ZA27 alloy hybrid composites and they stated that load has the primary impact factor on specific WR, followed by sliding speed and Gr content. Saravanan et al. [22] studied the tribological characteristics of TiO_2 particles filled aluminium 6063 alloy nano composites manufactured by liquid metallurgy route. They observed that the WR mainly dependent upon TiO_2 occurrence in the alloy and also the load has more dominant factor thus will enhance the WR. Donanta et al. [23] studied the mechanical properties on fabricated AMCs with presence of A356, SiC, and strontium. The wear and hardness were improved by the increasing of weight percentages in SiC at particular weight percentage. Abdul Aabid et al. [24] investigated the dry sliding wear behaviour of aluminium 2219 matrix composites reinforced with B_4C, MoS_2 and Gr particulates and reported that B_4C particles in the matrix increases the wear resistance of MMC when compared to ther particles. Siddesh Kumar et al. [25] studied the wear behaviour of Al2219 reinforced with B_4C and MoS_2 particulates MMCs and they reported that temperature, load and sliding velocity chiefly controlled the WR and also the addition of self lubricating MoS_2 content resisting against the WR. Justin Maria Hillary et al. [26] investigated the tribological behaviour of Al6061/SiC/TiB_2 hybrid composites produced via stir casting route. They observed that the COF linearly decreases with an increase in load and sliding distance. Similarly, at a lower sliding distance and sliding velocity, the wear resistance significantly improved. Alagarsamy et al. [27] investigated the effect of wear control parameters namely load, sliding velocity and sliding distance for the TiO_2 reinforced Al7075 alloy composites and reported that load has the most significant factor on reduced the WR and COF. Based on the above studies, an attempt was made to examine the effect of 10 wt.% TiO_2 addition on hardness and tribological behaviour for the AA8011 matrix composites manufactured by stir casting route. Furthermore, TOPSIS approach employed to find out the optimal conditions of dry sliding wear control parameters for obtain the less SWR and COF for the proposed composite. At last, the worn-out surface morphology of the tested composite specimen was studied by SEM to understand the wear mechanism.

2. Materials and methods

In this research work, aluminium 8xxx alloy (AA8011) was utilized as matrix material and it contains chemical compositions (wt.%) are Fe-1.0, Si-0.9, Mn-0.20, Cu-0.10, Zn-0.10, Mg-0.05, Cr-0.05, Ti-0.08 and Al-remaining. This alloy has been playing a vital role in automotive, aerospace and defence sectors due to their unique properties such as high strength, stiffness and high thermal stability. TiO_2 (Loba Chemie, Mumbai, India) was

used as reinforcement particles having a particle size of 5 µm, density of 4.9 g/cm^3, elastic modulus of 230 GPa and thermal conductivity of 4.8 W/m.K respectively. This reinforcement was chosen because TiO_2 particles are one of the most often utilised oxides because to its excellent wettability, great mechanical properties, and high wear and corrosion resistance. Bottom pouring type stir casting method was used to manufacture the composite. At first, pure ingot AA8011 was kept into graphite crucible then it was melted in electrical furnace at the temperature of 750°C. Meanwhile, the required amount of TiO_2 particles were preheated at 200°C [11] to remove the moisture and also to improve the wettability of the TiO_2 particles with molten AA8011. The molten AA8011 was stirred with a motorized agitator at the speed of 200 rpm constantly. Subsequently,

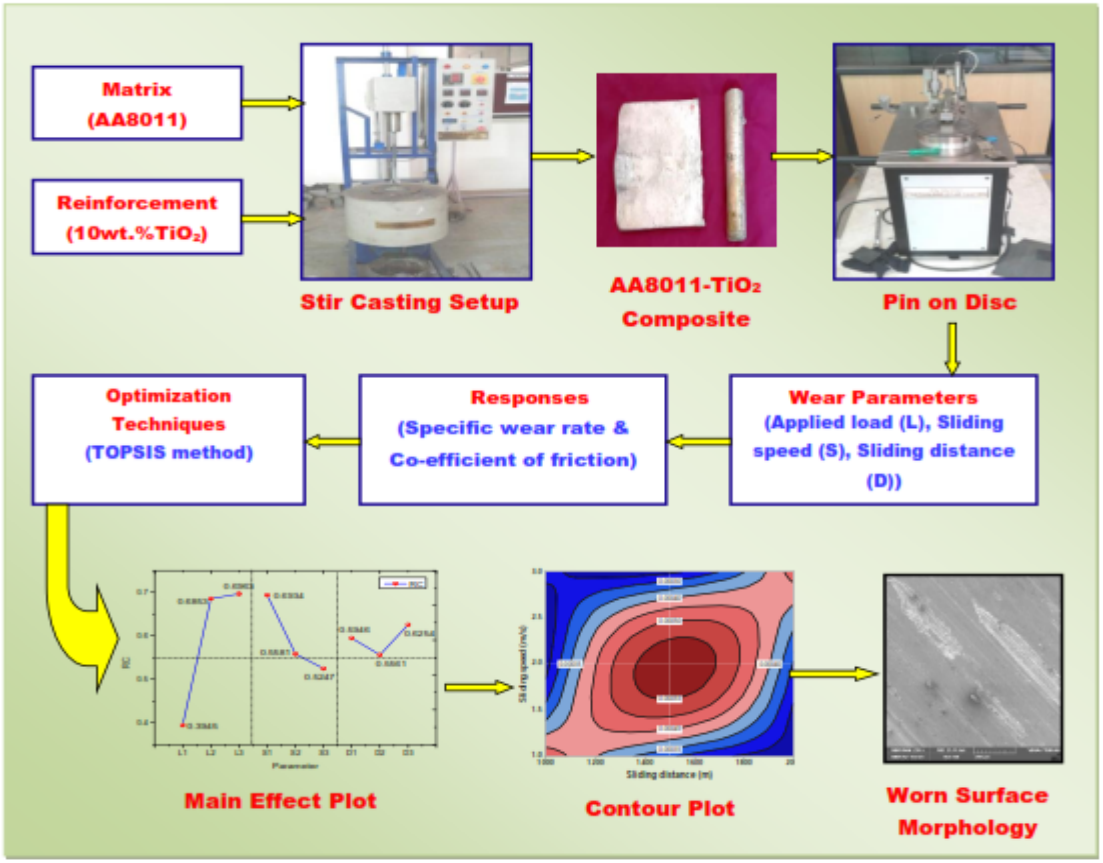

Fig. 1. Layout of experimental plan

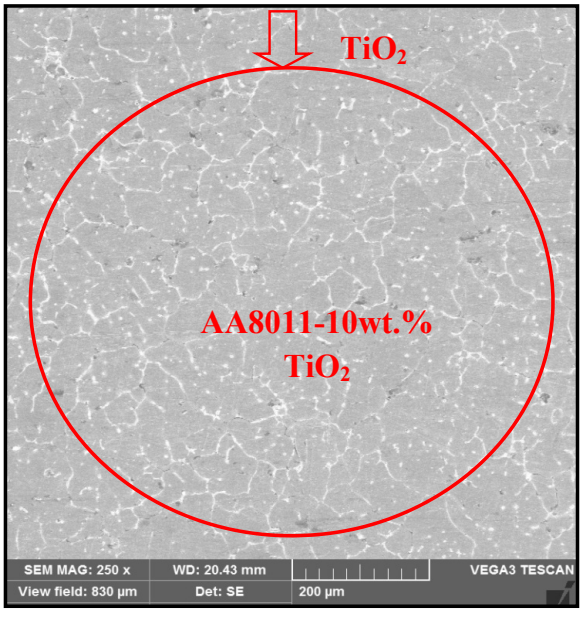

Fig. 2. SEM micrograph of the AA8011-10 wt.% TiO_2 composite

the preheated TiO_2 particles were slowly added in the vortex of the molten pool. To achieve a uniform distribution of particles in the AA8011 pool, then the mixture was constantly stirred at 250 rpm around 20 min [32]. Finally, the composite slurry was poured into the preheated mould directly. The required size of the specimen was prepared from the casted composite. Fig. 1 shows the experimental plan of present study. Scanning electron microscopy (Vega3, Tescan model) was used to taken the surface morphology of the proposed composite. Fig. 2 display the SEM micrograph of the manufactured AA8011-10 wt.% TiO_2 composite. It can be clearly seen from the graph is that the absence of agglomerations of TiO_2 particles and also it was ensured a homogeneous dispersion of TiO_2 particles within the AA8011 matrix. As per ASTM E98 standard the micro hardness was determined by using vicker's hardness tester. The maximum hardness was achieved at 95.6 Hv and it was greater than the unreinforced matrix alloy.

Here, the manufactured composite specimen was taken for studying the tribological behaviour such as SWR and COF

respectively. A pin on disc (TR-20 DUCOM) tribometer was used to perform the dry sliding wear test. The test pins were prepared from the casted composite as per ASTM G-99 standard with a dimension of 10 mm × 10 mm × 30 mm by using wire-cut electric discharge machine. From the earlier studies, there are many factors significantly affects the tribological behaviour of the composites. Among them, applied load, sliding speed and sliding distance are the key factors to control the SWR and COF [24]. Hence, in this investigation those three factors each at three levels were taken as input parameters and are depicted in TABLE 1. After that, the wear tests were performed as per L_9 (3^3) orthogonal array (OA) and are given in TABLE 2. The output responses like the SWR and COF was computed. To calculate the SWR, the initial and final mass of the specimen was weighted using an electronic weighing balance machine. The standard formula for SWR and COF as used elsewhere [25], and the values are depicted in TABLE 2.

TABLE 1

Wear control parameters and its levels

Wear Parameters	Unit	L_1	L_2	L_3
Applied load (L)	N	10	20	30
Sliding speed (S)	m/s	1	2	3
Sliding distance (D)	m	1000	1500	2000

TABLE 2

L9 (3^3) array table with experimental results

Exp. No.	Applied load (N)	Sliding speed (m/s)	Sliding distance (m)	Specific wear rate (mm^3/N-m)	COF
1	10	1	1000	0.000487	0.424
2	10	2	1500	0.000582	0.536
3	10	3	2000	0.000476	0.625
4	20	1	1500	0.000307	0.521
5	20	2	2000	0.000296	0.640
6	20	3	1000	0.000272	0.745
7	30	1	2000	0.000217	0.565
8	30	2	1000	0.000228	0.728
9	30	3	1500	0.000238	0.845

3. Optimization using TOPSIS Approach

Technique for Order Preference by Similarity to Ideal Preferred Solution (TOPSIS) approach is one of the most efficient methods employed in MCDM techniques. Hence, in order to optimize the control parameters on the response like SWR and COF. TOPSIS approach was applied in this investigation. This approach was introduced by Hwang and Yoon in 1981 to solve multi criteria decision making problems [26]. In this investigation, an L_9 orthogonal design was constructed to conduct the less number of experiments. During this approach, best solution is selected which should have shortest distance to the positive ideal solution and farthest to the negative ideal solution. The positive ideal solution is a solution that tries to maximize the profit criteria and minimizes the cost criteria, whereas negative ideal solution maximizes the cost criteria and minimizes the profit criteria [27]. The given steps to be implemented and are as follows,

Step1: The decision matrix D_{max} was constructed for the m alternatives and n attributes are as follows,

$$D = \begin{bmatrix} x_{11} & x_{12} & \cdots & \cdots & x_{1j} \\ x_{21} & x_{22} & \cdots & \cdots & x_{2n} \\ \cdots & \cdots & \cdots & \cdots & \cdots \\ x_{i1} & x_{i2} & \cdots & x_{ij} & x_{in} \\ \cdots & \cdots & \cdots & \cdots & \cdots \\ x_{m1} & x_{m2} & \cdots & x_{mj} & x_{mn} \end{bmatrix}$$

where, x_{ij} is the value of the optimal characteristics, where $i = 1 - m$ is the number of results of each characteristic, and $j = 1 - n$ is the number of characteristics to be optimized.

Step 2: The normalized decision matrix (r_{ij}) was computed. The output results were normalized in the range of 0 to 1 by using Eq. (1),

$$r_{ij} = \frac{x_{ij}}{\sqrt{\sum_{i=1}^{m} x_{ij}^2}} \tag{1}$$

where $i = 1,2,\ldots, m$ and $j = 1,2,\ldots, n$. x_{ij} denotes the actual value of the i^{th} value of j^{th} experiment.

Step 3: The weighted normalized decision matrix (v_{ij}) was calculated by using Eq. (2). In this analysis, we taken equal weights ($w_j = 0.5$) due to both responses are equally important.

$$v_{ij} = r_{ij} \times w_j \tag{2}$$

where, w_j denotes the weight of the j^{th} attribute, $w_j = 0.5$, $i = 1,2,\ldots, m$ and $j = 1,2,.., n$. The normalized and the weighted normalized matrix are provided in TABLE 3.

TABLE 3

Normalized and weighted normalized matrix

Exp. No.	Normalized matrix		Weighted normalized matrix	
	SWR	COF	SWR	COF
1	0.442004	0.221719	0.221002	0.110860
2	0.528227	0.280287	0.264113	0.140143
3	0.432020	0.326827	0.216010	0.163413
4	0.278635	0.272443	0.139317	0.136221
5	0.268651	0.334671	0.134326	0.167335
6	0.246869	0.389578	0.123434	0.194789
7	0.196950	0.295451	0.098475	0.147726
8	0.206934	0.380688	0.103467	0.190344
9	0.216010	0.441870	0.108005	0.220935

Step 4: The positive ideal solution (A^+) and the negative ideal solution (A^-) were calculated by using Eq. (3) & (4),

$$A^+ = \left\{ \sum_{i=1}^{\max} v_{ij} \Big/ j \in J, \sum_{i=1}^{\min} v_{ij} \Big/ j \in J' \right\} \tag{3}$$

$$A^{-} = \left\{ \min_{i=1} \sum v_{ij} \Big/ j \in J, \max_{i=1} \sum v_{ij} \Big/ j \in J' \right\} \quad (4)$$

where, J is associated with the benefit parameters and J' is associated with non-benefit parameters. TABLE 4 presented the positive and negative ideal solutions.

TABLE 4

Positive and negative ideal solutions

Response	A^{+}	A^{-}
SWR	0.098475	0.264113
COF	0.110860	0.220935

Step 5: The separation measures of each alternative from the positive and the negative ideal solution were computed by Euclidean distance by using the Eq. (5) & (6) and the values are given in Table 5.

$$S_i^{+} = \sqrt{\sum_{j=1}^{n} \left(v_{ij} - A^{+} \right)^2}, \quad i = 1, 2, \ldots, m \quad (5)$$

$$S_i^{-} = \sqrt{\sum_{j=1}^{n} \left(v_{ij} - A^{-} \right)^2}, \quad i = 1, 2, \ldots, m \quad (6)$$

Step 6: The relative closeness (C_i) value of each alternative to the ideal solution was determined by using Eq. (7) and the values are provided in TABLE 5.

$$C_i = \frac{S_i^{-}}{S_i^{+} + S_i^{-}} \quad (7)$$

TABLE 5

Separation measure and relative closeness

Exp. No.	Separation measure		Relative closeness (C_i)	Rank
	S_i^{+}	S_i^{-}		
1	0.122527	0.118217	0.491048	7
2	0.168207	0.080792	0.324466	9
3	0.128749	0.074984	0.368050	8
4	0.048076	0.150832	0.758300	2
5	0.066893	0.140420	0.677331	3
6	0.087561	0.143088	0.620370	5
7	0.036866	0.181095	0.830861	1
8	0.079641	0.163533	0.672495	4
9	0.110487	0.156108	0.585563	6

Relative closeness (C_i) value represented a single response by converted the multiple responses (i.e. SWR and COF). Fig. 3 shows the experiment number versus computed RC. From the graph, it has been stated that the greatest response was recognized according to the preference rank of higher RC value. It can be seen (Fig. 3) that the higher RC value is obtained at ex. no 7 which consists of an optimal conditions of parameter for getting less SWR and COF for the AA8011-10 wt.% TiO_2 composite developed via stir casting route.

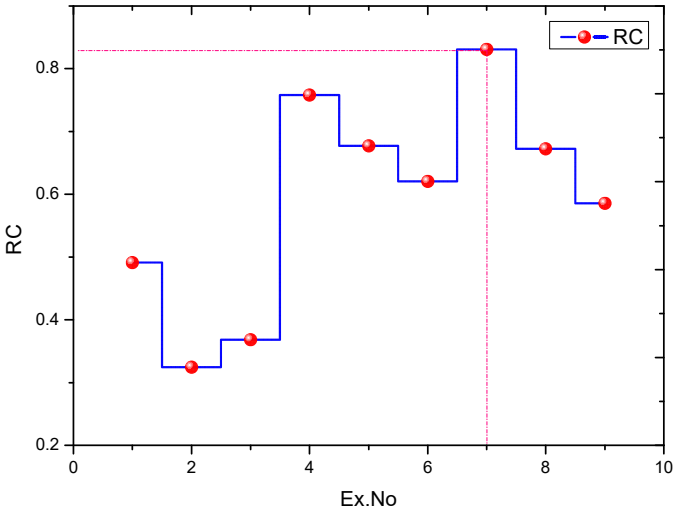

Fig. 3. Rank plot for relative closeness

4. Results and discussion

4.1. Effect of Control Parameters on Tribological Behaviour

The purpose of this research work was to find out the optimal combinations of control parameters for obtain the less SWR and COF on AA8011-10 wt.% TiO_2 composite under dry condition. In TOPSIS approach, multi-response characteristic like relative closeness (C_i) value was obtained from the single responses such as SWR and COF. Fig. 4 illustrates the effect of control parameters on mean relative closeness (C_i). In the Fig, the each level of input parameters such as applied load (L), sliding speed (S) and sliding distance (D) are denoted in x-axis, similarly the output response like mean of relative closeness (C_i) is provided in y-axis. Usually, the larger relative closeness (C_i) value of each parameter have considered as the optimal level. As seen in Fig. 4, it can be stated that the optimum condition of control parameters are applied load at level 3 (L_3 = 20 N), sliding speed at level 1 (S_1 = 1 m/s) and sliding distance at level 3 (D_3 = 2000 m) respectively. In general, the specific wear rate

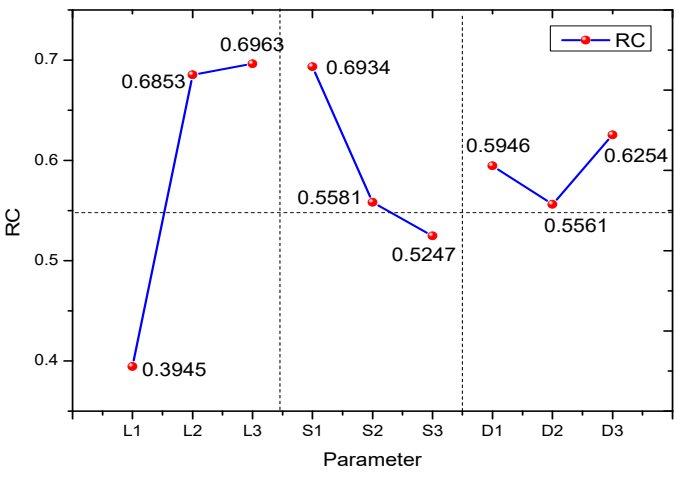

Fig. 4. Main effect plot for relative closeness

and COF mainly control by the. But, in this case the SWR and COF minimized at higher level of applied load (*L*) and sliding distance (*D*). The reason is behind that, the inclusion of TiO_2 particles improve the surface hardness of the manufactured composite thus will resists the more friction and wear loss from the specimen during rotation of the disc. The similar observations have been made by Alagarsamy et al. [28] while dry sliding wear behaviour analysis for AA7075-TiO_2 composite.

The mean table for relative closeness (C_i) with respect to individual level of control parameters are shown in TABLE 6. From the table, we can understood that the order of dominant factors on the response characteristics. The maximum value of delta represents the primary notable parameter which is stated as rank 1, subsequently by other parameters like rank 2 and 3 etc. As per the results (TABLE 6), it was clearly revealed that the applied load (*L*) has the most predominant factor on the response characteristics, followed by sliding speed (*S*) and sliding distance (*D*) respectively. The rise in load on the composite pin leads to high wear loss. Because an increase in applied load degrades the existing tribolayer which results in the transition from moderate to harsh wear loss occurs. The same observations was earlierly reported by Ajith et al. [29] during tribological wear test for aluminium 5059/SiC/MoS_2 hybrid composites. They stated that applied load and sliding distance were the most predominant factors on the responses.

TABLE 6

Means table for relative closeness

Level	*L* (N)	*S* (m/s)	*D* (m)	Average relative closeness (C_i)
1	0.3945	0.6934	0.5946	0.592054
2	0.6853	0.5581	0.5561	
3	0.6963	0.5247	0.6254	
Delta	0.3018	0.1687	0.0693	
Rank	1	2	3	

Fig. 5(a-c) illustrates the interaction effect of the wear control parameters namely applied load (L), sliding speed (S) and sliding distance (D) on the SWR of AA8011-10wt.% TiO_2 composite. In Fig. 5(a) shows the interaction of 'L' versus 'S' on SWR of the tested composite. It can be noticed that the SWR gradually decreasing with an increase in 'L'. Therefore, the low SWR of 0.00025 mm^3/N-m achieved at 30 N of 'L' with 2.0 m/s of 'S'. Generally, the SWR increases with an increasing in 'L'. In Fig. 5(b) demonstrates the effect of 'L' versus 'D' on SWR for the tested composite. Based on the graph, it is clearly noted that the SWR linearly decreasing with an increase in 'L'. The less SWR (0.00025 mm^3/N-m) is produced at middle level of 'D' (1500 m) with 25 N of 'L'. Usually, the SWR is directly proportional to the 'L'. However, in this investigation the higher SWR produced at maximum load conditions 30 N because of the addition of TiO_2 particles homogeneously distributed over the matrix alloy which resist the metal removal from the specimen surface. In Fig. 5(c) illustrates the interaction of 'S' versus 'D' on SWR of the developed composite. It can be reveal that the SWR increases with an increased in 'S' at moderate level of 'D' (1500 m). The initial level of 'D' (1000 m) with middle level of 'S' (2.0 m/s) produce minimum SWR (0.00035 mm^3/N-m) of the proposed composite.

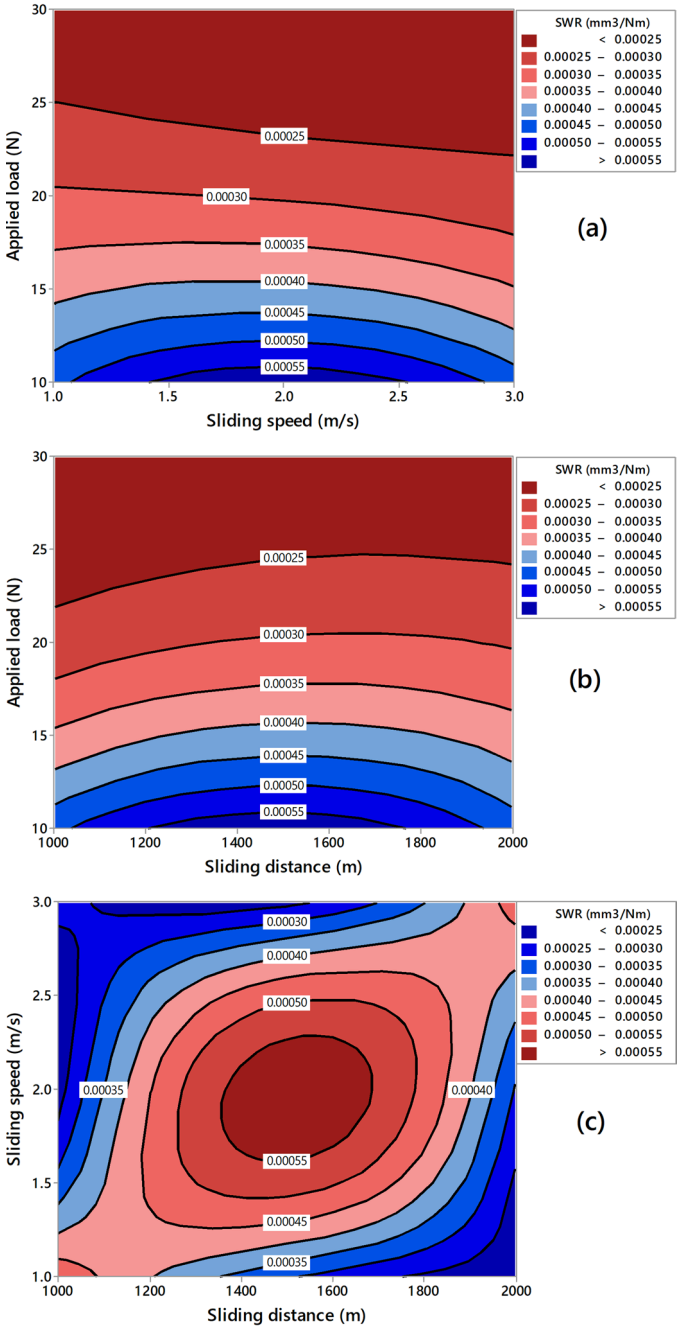

Fig. 5. Contour plot of SWR (a) *L* vs. *S*, (b) *L* vs. *D* and (c) *S* vs. *D*

Fig. 6(a-c) demonstrates the effect of control parameters namely applied load (*L*), sliding speed (*S*) and sliding distance (*D*) on the COF for the AA8011-10wt.% TiO_2 composite. In Fig. 6(a) clearly shows that the interaction of 'L' with 'S' on COF. The maximum COF (0.72) made at middle level of 'L' (20 N) with high level of 'S' (3.0 m/s). However, the low COF (0.54) produced at 20 N of 'L' with initial 'S' of 1.0 m/s respectively. Furthermore, an increase in 'L' decreasing the COF at all level of 'S'. The reason is behind that, the incorporation

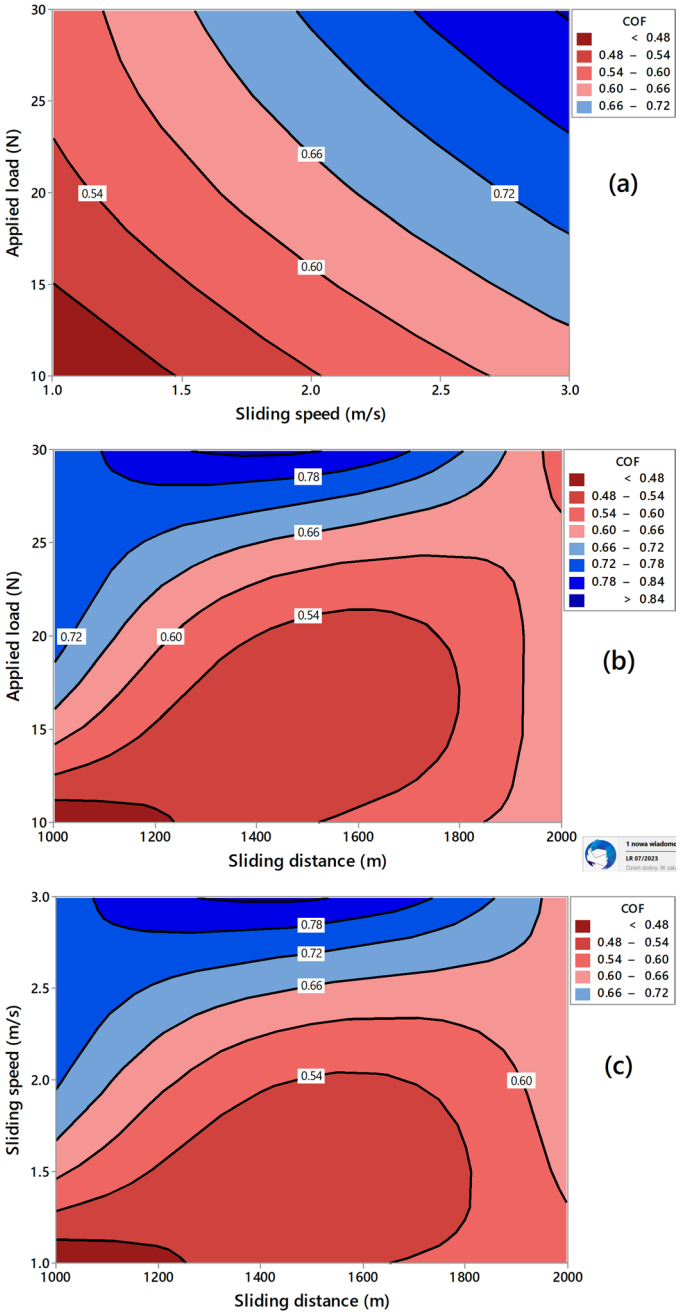

Fig. 6. Contour plot of COF (a) *L* vs. *S*, (b) *L* vs. *D* and (c) *S* vs. *D*

of TiO_2 particles improved the hardness of the matrix alloy which resists the friction against the specimen surface. Hence, the developed composite obtained less COF, thus will reduce the SWR. In Fig. 6(b) shows the effect of 'L' versus 'D' on the COF. From the graph, it is noted that the COF increasing with an increase in 'L' at higher level. However, the moderate 'D' (1500 m) with middle level of 'L' (20 N) produce less COF (0.54). At the same time, the maximum COF (0.72) made at middle level of 'L' (20 N) with initial level of 'D' (1000 m). The effect of 'S' with 'D' on COF is display in Fig. 6 (c). It is noticed that the COF gradually increasing with an increase in 'S' at middle level of 'D' (1500 m). Here, the high value of COF from 0.66 to 0.78 has produced at moderate level of 'D' (1500 m) with 'S' of 2.5 m/s to 3.0 m/s respectively.

4.2. Analysis of Variance (ANOVA)

ANOVA is a statistical tool extensively applied to identify the impact of process parameters on the response characteristics and also compute the percentage contribution of those parameters [30]. Hence, in this investigation an ANOVA was employed to determine the impact of control parameters namely 'L', 'S' and 'D' on the SWR and COF of the AA8011-10wt.% TiO_2 composite while dry sliding wear test. The ANOVA results are provided in TABLE 7 and also the graphical representation of parameters contribution plot is illustrates in Fig. 7. According to the TABLE 7, the F-ratio and P-value are used to show the significant parameters at 95% confidence level. The F-ratio of 'L', 'S' and 'D' are 522.87, 142.49 and 21.52 which are very higher than tabulated F-value ($F_{0.05,2,8} = 4.46$), and also the P-value of those parameters are less than 0.05, which confirmed that those parameters were significantly affecting the response characteristics. From Fig. 7, it has been clearly reveal that 'L' was the greater impact factor on the response with a contribution is 76.01%, subsequently by 'S' and 'D' with contributions are 20.71% and 3.12% respectively. The error was obtained at 0.145% only. The similar observations was reported earlier by Alagarsamy et al. [23] during dry sliding wear behaviour of AA7075-TiO_2 composites and concluded that applied load was the more noteworthy factor for influencing the tribological behaviour.

TABLE 7

ANOVA for relative closeness

Source	DF	Seq SS	Adj SS	Adj MS	F-Value	P-value
L	2	0.175766	0.175766	0.087883	522.87	0.002
S	2	0.047899	0.047899	0.023950	142.49	0.007
D	2	0.007235	0.007235	0.003617	21.52	0.044
Error	2	0.000336	0.000336	0.000168	—	—
Total	8	0.231236	—	—	—	—
S = 0.0129645; R-Sq = 99.85% ; R-Sq(adj) = 99.42%						

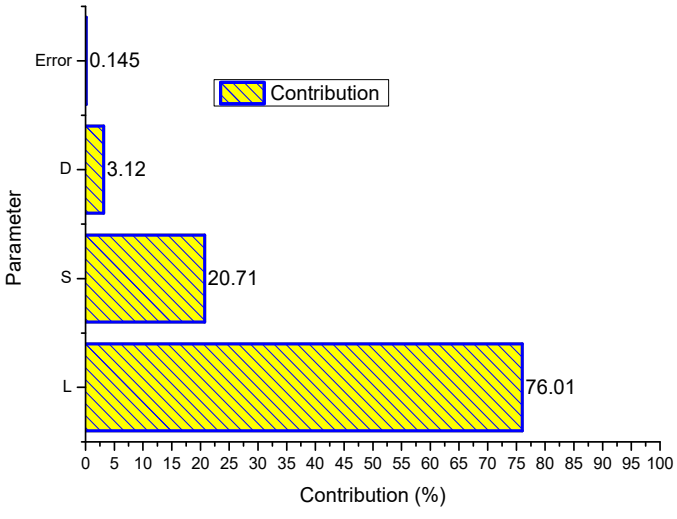

Fig. 7. Contribution plot of parameters

4.3. Confirmation experiments

To validate the predicted results, the confirmation experiment was taken out by the optimized parametric conditions as given in TABLE 8. The predicted value of the response characteristics was determined by given Eq. (9). [31]

$$\alpha_{pre} = \alpha_m + \sum_{k=1}^{n} (\alpha_i - \alpha_m) \tag{9}$$

where, α_{pre} – predicted value of response, α_m – total mean value of response, α_i – is response mean value at the optimum level and k – number of control parameters. From TABLE 8, it was showed that the relative closeness (C_i) values for the experimental and predicted values are 0.83086 and 0.83002 respectively. A very low percentage of error 0.002% was obtained between the experimental and predicted results which ensure the very good correlation. Fig. 8 displays the probability plot for relative closeness; it was noticed that the responses are located along the straight line, which confirms that the errors were normally distributed for the developed model.

TABLE 8

Confirmation experiments

Parameter setting	Optimal level	Specific wear rate (mm^3/Nm)	COF	Relative closeness (C_i)	Error (%)
Experimental	$L_3S_1D_3$	0.00217	0.565	0.83086	0.002
Predicted	$L_3S_1D_3$	—	—	0.83002	

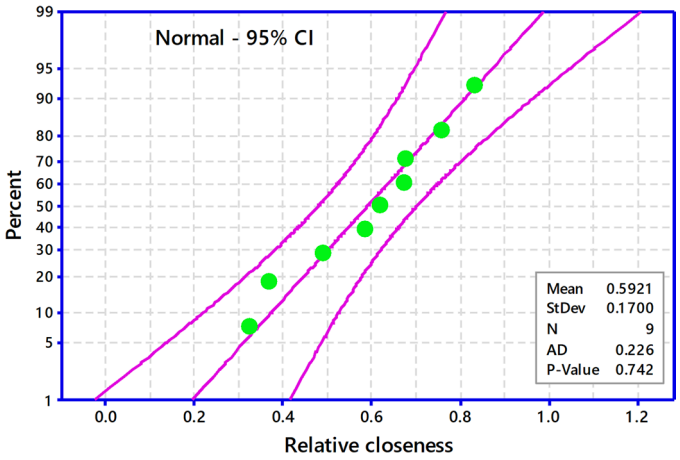

Fig. 8. Probability plot of RC

4.4. Worn Surface Morphology

Fig. 9(a & b) illustrates the worn out surface morphology of the tested AA8011-10 wt.% TiO_2 composite specimens at various conditions of wear control parameters. From the micrograph, it can be clearly understand the wear mechanism. Fig. 9(a) reveals the worn out surface of the initial parametric conditions are at a load of 10 N, sliding speed of 1 m/s and sliding distance of 1000 m respectively. It shows the occurrence of ploughs, grooves and delamination on the worn surface of the composite specimen. It is also clear that when the applied load increases, the SWR increases, as does the contact between the abrasive particles and the specimen, resulting in an increase in COF. By severe delamination with higher load, adhesion was produced. Dislodged particles occur in certain areas as a result of the recurrent sliding motion, and some debris has been removed from the ridges. Some pits emerge in the worn out surface due to the loss of reinforcing (TiO_2) particles. As a result, the abrasive mechanism is activated. When the hard TiO_2 reinforcement particles serve as load bearing components, then abrasive wear is conceivable at lower loads. In Fig. 9(b) illustrates the optimal parametric conditions of a worn out surface at a load of 30 N, sliding speed of 1 m/s and sliding distance of 2000 m respectively. The existence of a smooth surface as well as small grooves on the worn out surface was clearly visible. The micro crack appears in a few areas on the surface due to increased load (30 N) circumstances. The mechanical mixed layer (MML) is created as a result of material transfer between the counterpart and pin surface, resulting in a lower SWR and COF. Furthermore, the introduction of TiO_2 particles is the primary reason for increased wear resistance due to their higher hardness than the base alloy. The creation of an oxide layer between the abrasive wheel and the composite pin as the temperature rises. COF is reduced as a result of the creation of an oxide layer, which increases the composites wear resistance. Due to the contact between abrasive particles and the specimen surface at the shortest possible period for travelling the appropriate sliding speed, the creation of wear debris will be minimal as the sliding distance rises.

5. Conclusions

This research work was carried out to investigate the tribological behaviour of Al-0.6Fe-0.5Si alloy-TiO_2 composite. The following conclusions are taken out from this work:

1. AA8011 (Al-0.6Fe-0.5Si alloy) matrix reinforced with the composition of 10wt.% TiO_2 particles were successfully synthesized via stir casting route.
2. SEM micrograph of the manufactured composite ensured the addition of TiO_2 content homogeneously distributed within the matrix alloy. Hardness of the synthesized specimen was measured at different locations and found that the maximum hardness was obtained at 96.5 Hv.
3. The proposed composite was subjected to undergo the tribological wear test by using various levels of control parameters such as applied load (L), sliding speed (S) and sliding distance (D) and also the TOPSIS approach was employed to determine the optimum level of each parameter.
4. Based on the TOPSIS approach, the less specific wear rate and COF are obtained at the optimal combination of control parameters are L_3 = 30 N, S_1 = 1 m/s and D_3 = 2000 m respectively.

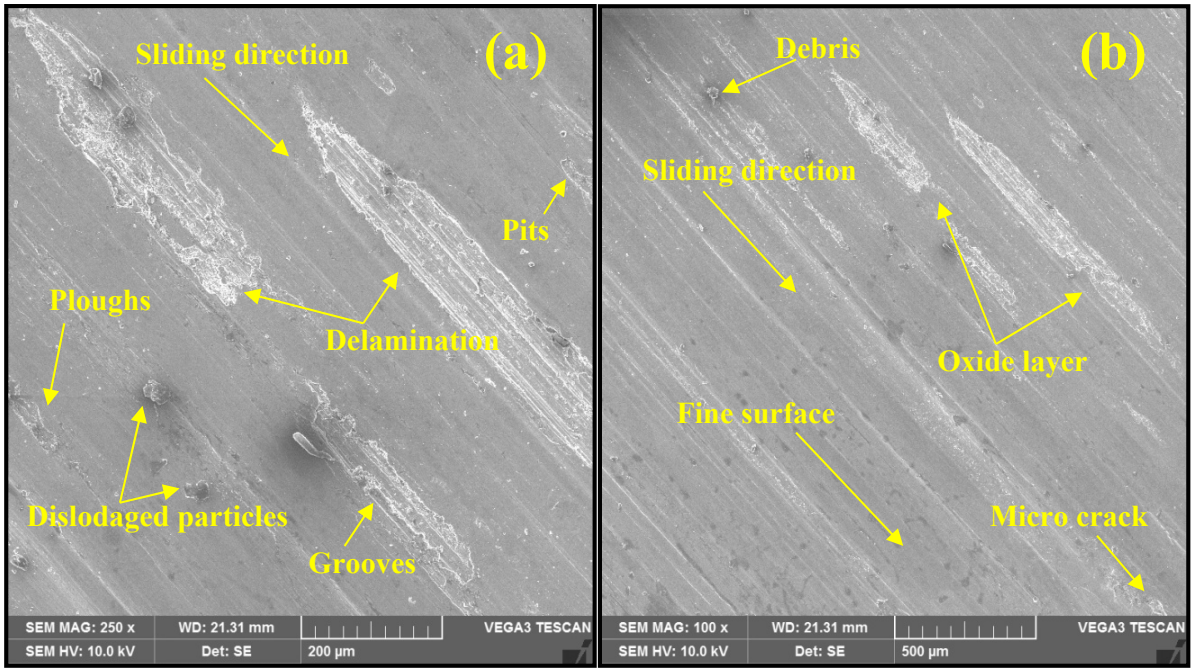

Fig. 9. SEM image of worn surface at (a) initial condition, and (b) optimal conditions of parameters

5. ANOVA result identified that applied load (*L*) was the most dominant factor with contribution is 76.01%, subsequently by sliding speed (*S*) and sliding distance (*D*) with contributions are 20.71% and 3.12% respectively.
6. Finally, the confirmation experiments were performed to validated the predicted results and found that an error is 0.002% only.
7. Wear mechanism was studied using SEM image of worn surface and it was revealed that the minimum wear loss is achieved due to addition of TiO_2 content formed the oxide layer.
8. In the future, nano particle size of TiO_2 reinforcements will be used to investigate the wear behaviour of AA8011 matrix composite. And also other optimization techniques such as machine learning algorithm and particle swarm optimization approach can be used in to optimize the parameters on SWR of the composite.

REFERENCES

[1] V. Mohanavel, M. Ravichandran, Mater. Test. **61**, 554-558 (2019).
[2] Mazahery M.O. Shabani, Ceram. Int. **38**, 1887-1895 (2012).
[3] S.L. Pramod, A.K.P. Rao, B.S. Murty, S.R. Bakshi, Mater. Des. **78**, 85-94 (2015).
[4] Supriya Nandy, Kalyan Kumar Ray, D. Debdulal, Mater. Sci. Eng A. **644**, 413-424 (2015).
[5] A. Baradeswaran, A. Elaya Perumal, Compos. B Eng. **54**, 146-152 (2013).
[6] D.E.J. Dhas, C. Velmurugan, K.L.D. Wins, K.P. Boopathi Raja, Ceram, Int. **45**, 614-621 (2019).
[7] R. Soundararajan, A. Ramesh, N. Mohanraj, N. Parthasarathi, J. Alloys. Compd. **685**, 533-545 (2016).
[8] E. Marin, M. Lekka, F. Andreatta, I. Fedrizzi, G. Itskos, A. Moutsatsou, N. Koukouzas, N. Kouloumbi, Mater. Charact. **69**, 16-30 (2012).
[9] Zeeshan Ahmad, Sabah Khan, Shabahat Hasan, J. Mater. Res. Technol. **9**, 9129-9135 (2020).
[10] S. Dhanalakshmi, N. Mohanasundararaju, P.G. Venkatekrishnan, Appl. Mech. Mater. **592-594**, 705-710 (2014).
[11] S.V. Alagarsamy, M. Ravichandran, Mater. Res. Express. **6**, 1-15 (2019).
[12] Tetsuro Yanaseko, Hiroshi Sato, Karla Mossi, Hiroshi Asanuma, Sens. Actuators A. Phys. **331**, 112518 (2020).
[13] Min Zeng, Hong Yan, Ke Li, Yushun Lei, J. Alloys. Compd. **897**, 163181 (2022).
[14] Subramanya R. Prabhu, Arun K. Shettigar, Mervin A. Herbert, Shrikantha S. Rao, Trans. Nonferrous. Met. Soc. China. **29**, 2229-2236 (2019).
[15] K.R. Ramkumar, S. Natarajan, J. Alloys. Compd. **93**, 526-532 (2019).
[16] Samuel O Akinwamide, Serge M Lemika, Babatunde A Obadele, Ojo J Akinribide, Bolanle T Abe, Peter A Olubambi, J. Compos. Mater. **53**, 3929-3938 (2019).
[17] J. David Raja Selvam, D.S. Robinson Smart, I. Dinaharan, Energy. Procedia. **34**, 637-646 (2013).
[18] Jaswinder Singh, Amit Chauhan, Trans. Nonferrous. Met. Soc. China. **27**, 2573-2586 (2017).
[19] X. Roshan Xavier, S. Julyes Jaisingh, J. Mech. Sci. Technol. **35**, 4917-4924 (2021).
[20] K. Raju, M. Balakrishnan, Silicon. **14**, 115-125 (2022).
[21] Nenad Miloradovic, Rodoljub Vujanac, Blaza Stojanovic, Ana Pavlovic, Compos. Struct. **264**, 113658 (2021).
[22] S. Saravanan, S.T. Jayasuthahar, V. Dhinakaran, S. Sankar, AIP. Conf. Proc. **2283**, 1-6 (2021).

[23] Donanta Dhaneswara, Anne Zulfia Syahrial, Muhammad Tsabit Ayman, Procedia. Eng. **216**, 43-50 (2017).
[24] N.G. Siddesh Kumar, R. Suresh, G.S. Shiva Shankar, Compos. Commun. **19**, 61-73 (2020)
[25] J. Justin Maria Hillary, R.Ramamoorthi, Samson Jerold Samuel Chelladurai, Mater. Res. Express. **7**, 1-16 (2020)
[26] Abdul Aabid, Mohammed Ali Murtuza, Sher Afghan Khan, Muneer Baig, J. Mater. Res. Technol. **16**, 743-763 (2022).
[27] S.V. Alagarsamy, M. Ravichandran, Ind. Lubr. Tribol. **71**, 1064-1071 (2019).
[28] S. Baskaran, V. Anandakrishnan, M. Duraiselvam, Mater. Des. **60**, 184-192 (2014).
[29] S. Thirumalai Kumaran, M. Uthayakumar, S. Aravindan, Tribol. **8**, 187-193 (2014).
[30] S.V. Alagarsamy, P. Raveendran, M. Ravichandran, Silicon. **13**, 2529-2543 (2020).
[31] A. Karthikeyan, S.V. Alagarsamy, C.Ilaiyaperumal. Surf. Rev. Lett. **29**, 1-11 (2021).
[32] S.V. Alagarsamy, M. Ravichandran, Mater. Res. Express. **7**, 1-17 (2020).
[33] Ajith Arul Daniel, Sakthivel Murugesan, Manojkumar, Sudhagar Sukkasamy, Mater. Res. **20**, 1697-1706 (2017).
[34] P. Raveendran, S.V. Alagarsamy, C. Chanakyan, M. Meignana-moorthy, M. Ravichandran, S. Sakthivelu, Surf. Topogr: Metrol. Prop. **9**, 1-12 (2021).
[35] Sakip Koksal, Ferit Ficici, Ramazan Kayikci, Omer Savas, Mater. Des. **42**, 124-130 (2012).